

BUILDING DETECTION AND STRUCTURE LINE EXTRACTION FROM AIRBORNE LIDAR DATA

C. K. Wang^a, P.H. Hsu^a *

^a Dept. of Geomatics, National Cheng Kung University, No.1, University Road, Tainan 701, Taiwan. China-
(p6896102, pahui)@mail.ncku.edu.tw

Commission III, WG III/3

Keywords: Laser scanning, Edge detection, Aerial Survey, Feature extraction, Buildings

ABSTRACT:

The development of LIDAR (Light Detection and Ranging) system makes the acquisition of 3D surface information more convenient and immediate than other geomatics technologies. However, the 3D coordinates of the surface features, such as the corners, edges and planes of buildings, cannot be obtained directly from the LIDAR data because of its blind characteristics. How to detect the feature locations effectively and further to reconstruct the building from the LIDAR point clouds becomes one of the most important applications and study issues. For this reason, an approach for building detection and feature lines extraction from airborne LiDAR data is proposed in this paper. The building detection is based on wavelet transform and geometric properties of buildings, and the extraction of feature lines is based on Hough transform and image processing. For data-driven building reconstruction, the feature lines are essential to reconstruct the roof models. The basic idea of the proposed approach is to detect the location of each single building in the raw LiDAR data firstly. Then, the initial feature lines which are divided into external contour lines and internal structure lines are extracted respectively. These structure lines could be provided as the features for data-driven building reconstruction. The experiment results showed that the feature lines of regular and simple roofs such as rectangle roofs, gabled roofs and L-type roofs could be extracted successfully.

1. INTRODUCTION

Building extraction and reconstruction from the measurement data has been a major subject in photogrammetry and remote sensing. Many building reconstruction methods have been presented in the past few years. The traditional method is to extract buildings manually. Although it can obtain high quality building models, it is both time-consuming and labour-consuming. Subsequently due to the development of digital photogrammetry, the methods of building detection and feature extraction based on the feature matching are also presented. For example, the edges in the images can be detected firstly and then the feature line matching method is used to obtain the structure lines of buildings. In recent years, due to the development of Airborne LiDAR (Light Detection and Ranging) system, the DEM and DSM can be obtained easily and quickly. And therefore many researchers develop their methods toward the LiDAR Data. The Airborne LiDAR system measures three-dimensional points over the surfaces of the terrain, buildings, trees and other objects. However, the 3D coordinates of the surface features cannot be obtained directly from the LiDAR data because of its blind characteristics. Brenner (2005) discussed many practical cases about building reconstruction using aerial images and LiDAR data. Besides, the variant data fusion is usually considered to reconstruct buildings. It is very beneficial to recognize a building by combining the complementary properties of laser scanning data and images, such as combining high-resolution satellite images with airborne laser scanner, and fusion of LiDAR data and aerial imagery to automatically reconstruct the buildings (Hongjian and Shiqiang, 2006). However, the auxiliary data corresponding to LiDAR data is not available always. In this paper, our

interesting focuses on the extraction of feature lines for the roof reconstruction from LiDAR data. Another one of our objectives is to verify if the buildings could be reconstructed successfully and efficiently only using LiDAR data.

2. BUILDING DETECTION

Building detection are usually performed before building reconstruction while the ground plane is not available or the existing databases is the potential occurrence of errors as well as their prospective lack of actuality and incompleteness. The Many detection methods using variety measuring data have been proposed. For example, the data fusion of CIR (colored infrared) imagery and LiDAR data for classification technique can be used to separate buildings from other categories (Haala and Brenner, 1999). Besides using the roughness of surfaces, the man-made structures can be easily discriminated from natural objects (Brunn and Weidner, 1997; Chen, Teo et al., 2005).

In this paper, the locations of buildings are firstly detected and every single area occupied by an independent building is obtained. Then the structure lines are extracted from these detected areas. Figure 1 shows the flow chart of our scheme. The approach for building detection is mainly based on the multi-resolution analysis which is carried out by 2D wavelet transform. Multi-resolution is an analysis technique which can decompose the original data (signals or images etc.) into different approximations with different resolutions. In Figure 2, the raw LiDAR data was interpolated into 2D range image firstly. Subsequently, by using 2D wavelet transform, the

* Corresponding author.

approximations corresponding to the original range image in coarser resolution were produced (see Figure 3 (a)). Notice that the details such as small objects and the single tree would be smoothed and the remaining were huge buildings, dense trees or other big objects. Figure 3(b) shows the result after performing the operation of edge detection. It is obvious that the edges of small objects disappeared gradually in the coarser resolution. More details about multi-resolution analysis for building detection can be seen in (Wang and Hsu, 2006).

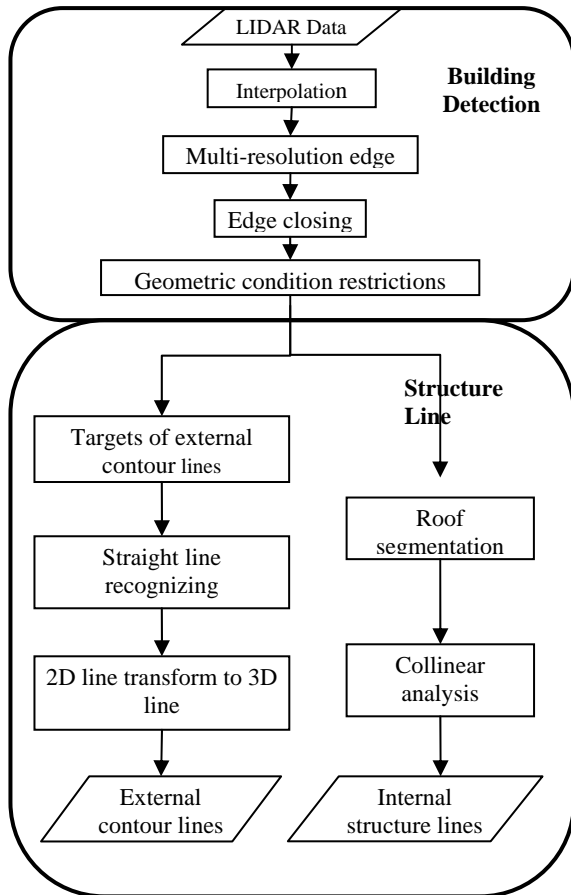


Figure 1. Flow chart of whole scheme

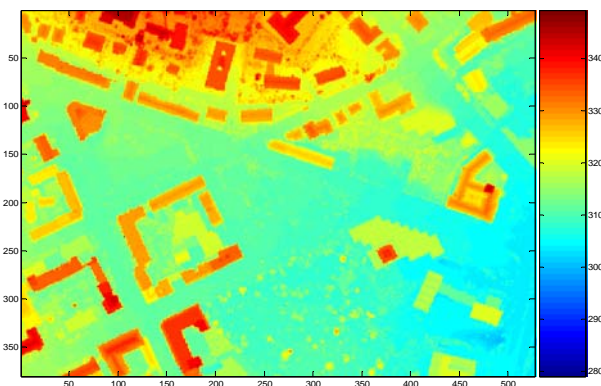
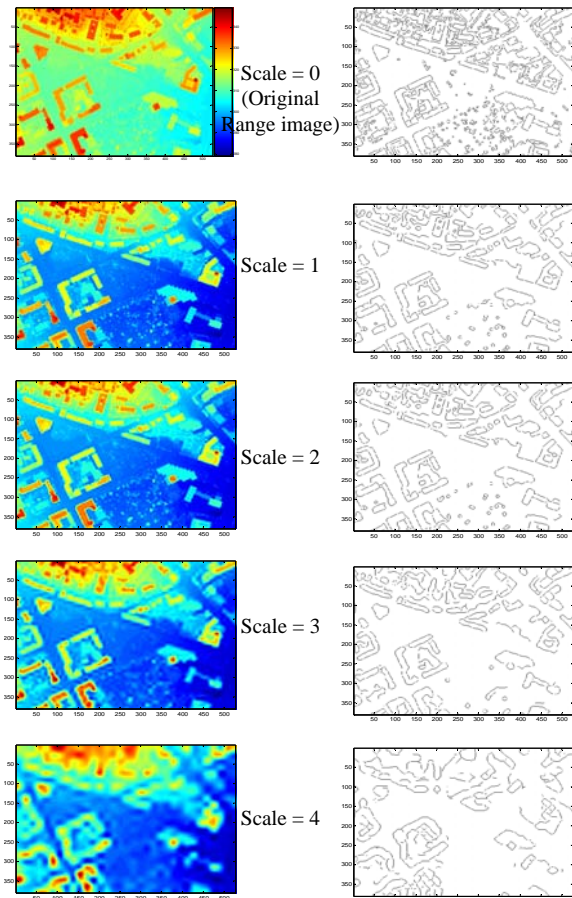


Figure 2. Range image

After obtaining multi-edges, the edges of objects on scale 2 was chosen. Then the morphology operator, closing operator which is composed of dilation and erosion, was used to enclose the broken edges. Accordingly the initial locations of buildings can

be determined by searching the closed curves. Figure 4 shows the result after searching closed curves. It is obvious that there were still non-buildings in Figure 4, therefore some geometric conditions of buildings were used to remove the objects of non-buildings. Firstly, the differences of the elevations between buildings and ground surfaces can be used to recognize and further to remove the ground pixels if the nDSM (Normalized Digital Surface model) was available. For this purpose, the goal is to produce the nDSM. As we mentioned before, the huge objects as well as the small objects could be smoothed on coarser resolutions and the approximation would be similar to the ground surface. So the approximation was used to substitute the DTM (Digital Terrain Model). And the DSM can be obtained from the original interpolated image. The nDSM was therefore calculated by the subtraction of DSM and DTM. Figure 5 shows the result after removing the ground pixels.



(a) Approximations in different scale

(b) The edges corresponding to the approximations

Figure 3. The approximations and the edges on different scales



Figure 4. The result of searching closed curves

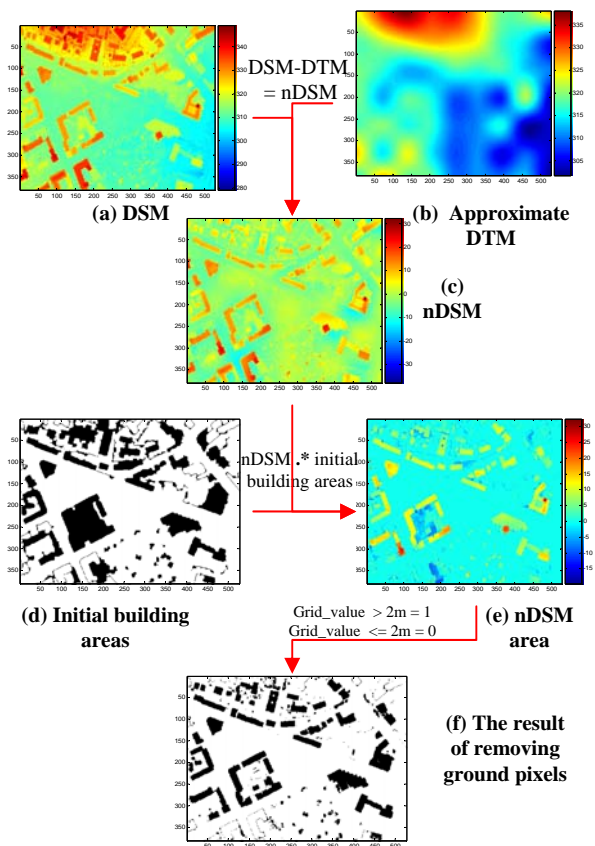


Figure 5. The procedure of removing ground pixels

Secondly the area of a building was supposed to be larger than a threshold. The objects which have small areas were therefore eliminated. Finally since the texture of buildings is different from others, the roughness values of every remaining object were computed in order to eliminate the non-buildings. Figure 6 shows the detecting results, (a) is the perspective image before performing detection method and (b) is the perspective image after performing detection method.

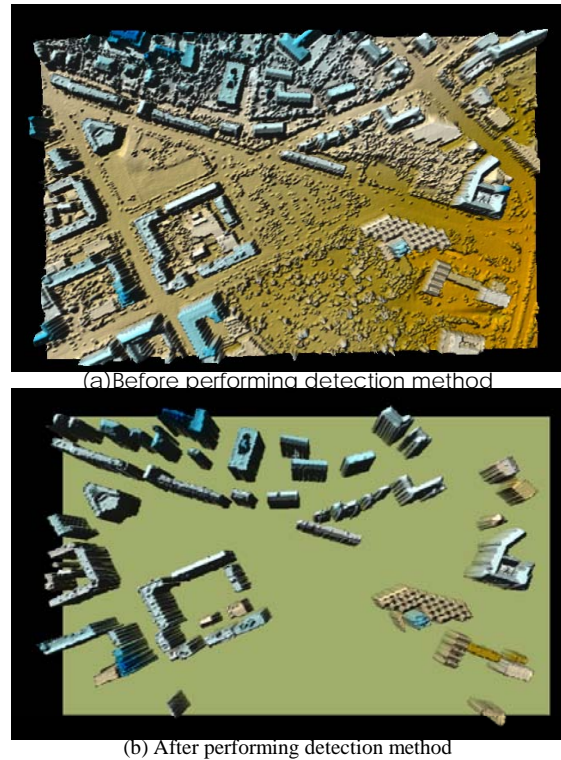


Figure 6. Building detection results

3. STRUCTURE LINE EXTRACTION

After building detection, the structure line extraction approach was performed on every single building. The structure line extraction approach is to extract the feature lines of roofs which are divided into external contour lines and internal structure lines in this paper.

3.1 External contour lines

In this section, our goal is to recognize the neighbour edge pixels as straight lines. For this reason, the roof borders were firstly searched and then were recognized as straight lines using Hough transform:

$$r = x \cos \theta + y \sin \theta \quad (1)$$

Figure 7 shows several examples of the recognition results. The buildings which have simple shape structures could be recognized successfully. However there were still failures (Figure (d)) due to the complicated structures. This usually happens while the edges are short or curved. While the contour lines were recognized, the elevation of every contour line must be given. We suppose that every line is on a level plane which means a contour line has only one elevation value only. And the elevation was acquired from the LiDAR points of roofs.

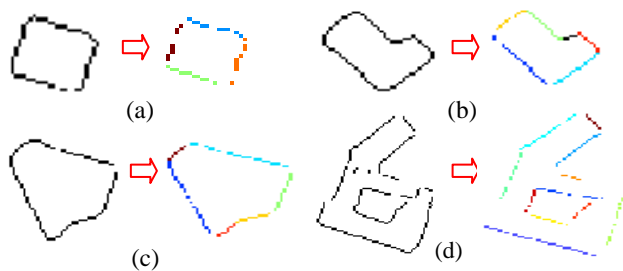


Figure 7. Four examples of contour line recognition, the black edges are unrecognized and the colourful edges are recognized.

3.2 Internal structure line

The internal structure lines were produced from the intersection of the connected faces if the faces of the roofs could be obtained. For this purpose, the LiDAR points of the roofs would be filtered and organized by Triangulated Irregular Network (TIN). Each face of a roof could be therefore segmented using region growing method since the normal vectors of grids in the same face are similar. Figure 8 shows one example of the whole procedure for extracting internal structure lines.

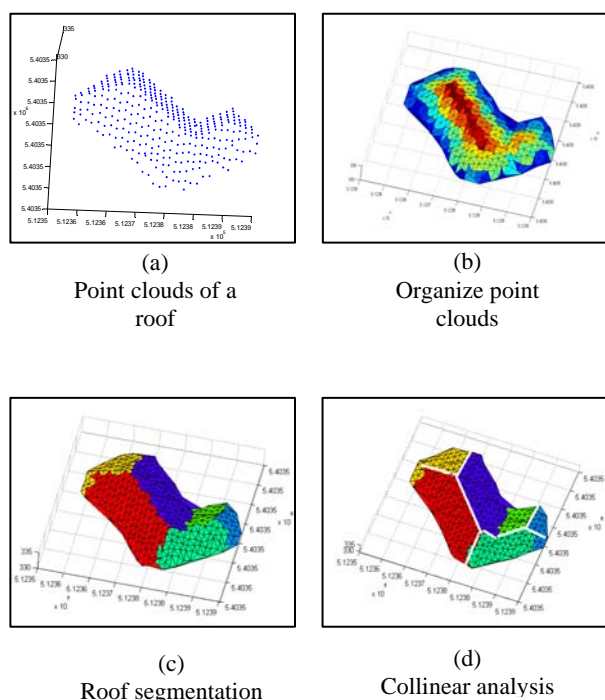


Figure 8. One example of the whole procedure of extracting internal structure lines

4. EXPERIMENT RESULTS

The test data is provided for free from ISPRS Commission III (<http://www.commission3.isprs.org/wg3/>). The site 3 data was chosen and the flying areas were over the Vaihingen/Enz test field and Stuttgart city centre in southern Germany. The point spacing is 0.67 points per square metre. The following shows the results of building detection and extracted lines.

4.1 Building detection results

The 3D perspective image of building detection is shown in Figure 6. Table 1 describes the ratio of successful detecting and miss-detecting. The failures in building detection were caused by the lower elevation of buildings, buildings mix with trees and the unsuccessful closing operator. The buildings would be removed while the difference of buildings and grounds is smaller than a threshold. Besides, the buildings which mix with trees would be retained since the roughness value is smaller than a threshold and could not be removed by the texture. The unsuccessful closing operator would cause the initial building searching to fail.

| | |
|---|--------------|
| Total number of buildings | 61 |
| Successive detected buildings/(percentage) | 53 / (86.9%) |
| Miss-detected buildings due to lower elevation/(percentage) | 6 / (9.9%) |
| Miss-detected buildings due to buildings mix with trees/(percentage) | 1 / (1.6%) |
| Miss-detected buildings due to the failure of closing operator/(percentage) | 1 / (1.6%) |

Table 1. Ratio of successful detecting and miss-detecting

4.2 Structure line extraction results

Table 2 shows the external contour line extraction results. The factors of the failures for extracting are:

1. Imperfect of edge detection: the external contour lines would not be extracted if they did not be detected during edge detection. Figure 9 explains this situation. The area in \bigcirc of Figure 9 should has a line to enclose the convex but the line did not be detected.
2. Failures of Hough transform: the straight line could not be recognized if the line is too short. It is because the parameters of Hough transform could not be suitable for the short lines.

| | |
|--|--------------|
| Total number of detected buildings | 54 |
| Successive extracted buildings / (percentage) | 37 / (68.5%) |
| Failures due to the imperfect of edge detection / (percentage) | 10 / (18.5%) |
| Failures of Hough transform / (percentage) | 7 / (13%) |

Table 2. Ratio of external contour line extraction

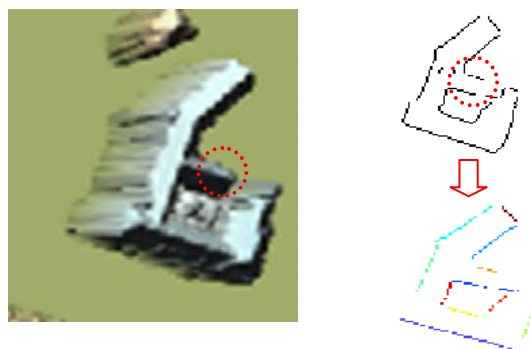


Figure 9. Imperfect of edge detection

Table 3 shows the internal structure line extraction results. The factors of the failures for extracting are:

1. Imperfect organizing: the structures of the organized points are different from real structures. ↓ in Figure 10 describes this situation, the redundant line would be produced due to the incorrect organized structures.
2. Other objects on the roof: the unexpected lines would be extracted while other objects are on the roof.
3. Imperfect region growing: the region growing may fail in the case of complicated structures of a roof. ○ in Figure 10 describes this situation.

| | |
|--|--------------|
| Total number of non-plane roofs | 26 |
| Successive extracted internal structure lines / (percentage) | 15 / (57.7%) |
| Failures due to the imperfect organizing / / (percentage) | 5 / (15.4%) |
| Failures due to other objects locating one the roof / (percentage) | 3 / (11.5%) |
| Failures due to the imperfect region growing / (percentage) | 4 / (15.4%) |

Table 3. Ratio of internal structure line extraction

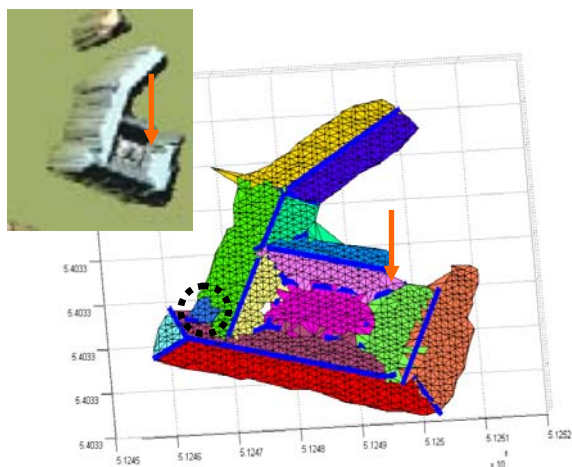


Figure 10. The factors of the failures for extracting

Figure 11 shows the results of the two feature line extraction. The green lines are external contour lines and the red lines are internal structure lines. From the results, both of the feature lines could be extracted successfully in the simple types of roofs. However there are many redundant or incorrect internal structure lines which were produced in the complicated structures.

4.3 Estimation of extracted lines

To estimate the extracted lines, another test area data at Hsinchu City, Taiwan is used for convenient. Figure 11 shows the extracted lines (red lines) which project to the aerial image. The coordinates of four corners were measured by GPS. The estimation method is to compute the coordinates of intersection points by extending the extracted lines and then compare the intersection points with GPS coordinates. The RMSE of the coordinates of the corners are shown in table 4.

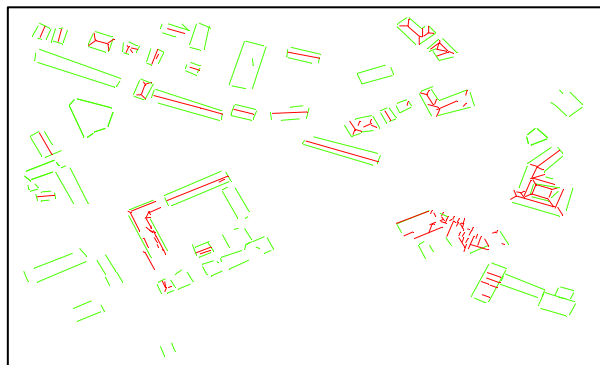


Figure 11. The results of structure line extraction

5. CONCLUSIONS

This paper presents a framework of building detection and feature line extraction. The experiments showed that most of the large buildings could be detected successfully and the structure lines of simple types of roofs could also be extracted successfully. The further research is to improve the structure line extraction of complicated roof structures and to combine the feature lines to reconstruct the roofs.



Figure 11. Projection of extracted lines on the aerial image

| RMSE_dX | RMSE_dY | RMSE_dZ | RMSE_total |
|---------|---------|---------|------------|
| 0.69 | 0.43 | 0.25 | 0.79 |

Table 4. RMSE of the estimated corners

The wavelet transform in building detection had two contributions. One is to avoid detecting edges of small objects and the other one is producing an approximate DTM in order to calculate the nDSM. From the results, the successful detection ratio is 86.9%. The failures were caused by the lower buildings significantly. In the aspect of external contour line and internal structure line extraction, the successful extraction ratios are 68.5% and 57.7% respectively. For external contour lines, the major influence factor is the completeness of original edges in the image. For internal structure lines, the major influence factor is the reality of the organized structures and the efficacy of region growing. For automatic topic, the human intervention is only required when the parameters or thresholds are needed to be determined. However, the adaptive parameter choosing is still an important issue of further research.

REFERENCE

- Brenner, C. (2005). "Building reconstruction from images and laser scanning." *International Journal of Applied Earth Observation and Geoinformation* 6(3-4), pp. 187-198.
- Brunn, A. and U. Weidner (1997). Extracting buildings from digital surface models. IAPRS.
- Chen, L.C., T.A. Teo, et al. (2005). Building Reconstruction from LIDAR Data and Aerial Imagery. *Geoscience and Remote Sensing Symposiu, IGARSS '05. Proceedings, 2005 IEEE International*, pp. 2846-2849.
- Haala, N. and C. Brenner (1999). Extraction of buildings and trees in urban environments. *ISPRS Journal of Photogrammetry and Remote Sensing* 54(2-3), pp. 130-137.
- Hongjian, Y. and Z. Shiqiang (2006). 3D building reconstruction from aerial CCD image and sparse laser sample data. *Optics and Lasers in Engineering* 44(6), pp. 555-566.
- Wang, C.K. and P.H. Hsu (2006). Building Extraction from LiDAR Data Using Wavelet Analysis. *Proceeding of 27th Asian Conference on Remote Sensing, Ulaanbaatar, Mongolia.*